THE UNIVERSITY of EDINBURGH

Edinburgh Research Explorer

Argon cluster impacts on layered silicon, silica, and graphite surfaces

OPEN ACCESS

Argon cluster impacts on layered silicon, silica, and graphite surfaces

J. Samela[1,a], K. Nordlund[1], J. Keinonen[1], V.N. Popok[2], and E.E.B. Campbell[2]

[1] University of Helsinki, Accelerator Laboratory, P.O. Box 43, 00014 University of Helsinki, Finland
[2] Gothenburg University, Department of Physics, 41296 Gothenburg, Sweden

Abstract. Seven structures of covalently bonded materials are used as targets of 6 keV Ar_{12} cluster bombardment in classical molecular dynamics simulations. Energy deposition, cratering and Ar ranges are compared and remarkable differences are found between the structures. In particular, bombardment of a thin 2 nm silica layer on top of the Si(111) surface is shown to behave quite differently from bombardment of pure Si.

1 Introduction

Ion and cluster impacts on covalently bonded materials have been studied intensively using molecular dynamics simulations (Ref. [1] and references therein). Most of the simulations have been done using ideal surfaces of pure crystals or amorphous targets. However, real surfaces are usually rough and can have oxide or amorphous layers. Such layers and roughness should be included in the simulation models in order to compare results of simulations to experimental measurements.

We have developed molecular dynamics models to simulate cluster impacts onto layered targets. In the next phase the results will be compared to experiments on keV-energy implantation of rare gas clusters into SiO_2/Si and HOPG (highly oriented pyrolytic graphite) targets. Surface smoothing by cluster bombardment was observed already in 1989 [2,3]. Now scanning probe and transmission electron microscopies provide a new opportunity to measure surface structuring on an atomic level [4–6]. The aim is to understand both qualitatively and quantitatively the emergence of various surface structures like craters, rims, hillocks, and bridges, as well as changes in surface roughness due to cluster impacts. In addition to the overall interest in collision cascade dynamics, the quantitative knowledge of surface changes could help in developing new applications of cluster bombardment and to further develop the existing techniques like surface smoothing.

2 Simulation methods

All simulations are carried out using classical molecular dynamics (MD). The simulation arrangements and suitability for cluster and ion bombardment simulations are discussed in references [7,8]. Here we summarize the simulation features, which are essential for the point of view of this paper.

Seven different target materials were simulated, all bombarded with 6 keV Ar_{12} clusters. The targets were chosen to represent common covalently bonded materials and layer structures. The targets are crystalline silicon (c-Si), amorphous silicon (a-Si), crystalline silicon with an approximately 2 nm thick amorphous layer (a-Si/c-Si), beta quartz (c-SiO_2), amorphous silica (a-SiO_2), crystalline silicon with an about 2 nm amorphous silica layer (a-SiO_2/c-Si), and graphite. For crystalline silicon, the (111) surface was used in the simulations as the target surface. Amorphous structures were prepared using MD by first melting the crystalline material and letting it cool down to an amorphous structure. All structures and their surfaces were relaxed at 300 K and zero pressure before bombardment. For each structure five simulations were carried out by altering only the impact point and the initial orientation of the cluster randomly.

The sizes of rectangular simulation boxes were chosen to be large enough to include whole collision cascades and to prevent boundary effects from distorting the cascades. The arrangement is discussed in reference [8]. The sizes of targets and simulation times are shown in Table 1. At the ends of the simulations no movement of atoms or sputtering was observed, but some elastic oscillations were still present in the graphite and silica targets.

a e-mail: juha.samela@helsinki.fi

**Table 1.** The numbers of atoms and target sizes in the simulations.

Target	Atoms	Box size (nm)	Simulation time (ps)
c-Si	1013760	$31 \times 32 \times 21$	30
a-Si	1013760	$31 \times 33 \times 21$	20
a-Si/c-Si	64812	$12 \times 12 \times 8$	30
c-SiO$_2$	29700	$10 \times 10 \times 8$	3
a-SiO$_2$	29700	$10 \times 10 \times 8$	2.5
a-SiO$_2$/c-Si	47530	$10 \times 10 \times 11$	10
Graphite	864012	$20 \times 20 \times 20$	50

A modified version of the Stillinger-Weber potential [9] was applied for the pure silicon structures to better describe the amorphous targets and layers. The modifications are obtained by fitting the potential parameters to produce experimental vibrational modes of the amorphous silicon structure. The potential is not the best choice for simulations of sputtering from c-Si, but it describes the amorphous phase well [9] and gives cascade depths that are comparable to depths obtained using other silicon potentials [7]. Silica targets were simulated with a version of the Stillinger-Weber potential [10,11] which is extended to include O-Si-O bonding. This potential gives a poor description of stress for compressively strained SiO$_2$ structures [12]. However, we found that the potential describes amorphous silica networks in close agreement with experimental pair correlation and bond angle data, although a steric hindrance in the potential yields a less dense structure than the real structure. The average O-Si bond length is 1.65 Å (experimental 1.609 Å), the average bond angle for O-Si-O is 142.3° (108.7°), and the average bond angle for Si-O-Si is 142.0° (148−152°) [13,14]. An improved Tersoff potential [15] was used in the graphite simulations. Argon clusters were prepared using a Lennard-Jones potential. Only a repulsive interaction between argon and the other elements was present [16].

3 Results and discussion

Energy deposition is analyzed by calculating the number of atoms that have been displaced from their original positions more than the thermal vibration amplitude during simulation. A small number of displaced atoms indicates that a larger portion of the cluster energy is deposited through elastic waves. The depth distributions of displaced atoms indicate how deep the deformations and defects are located.

Many effects of cluster collisions on solid structures, like crater formation, depend on the elastic properties of the atomic level environment around the collision cascade, which consists of liquid and void regions near the impact point and around the cluster track inside the solid. For example, Figure 1 shows the differences in cratering between homogeneous a-Si and a network of tetrahedral SiO$_4$ modules in a-SiO$_2$. The latter is well recovered from the collision and no visible crater is left. However, almost equally many target atoms have been displaced in both cases, as is
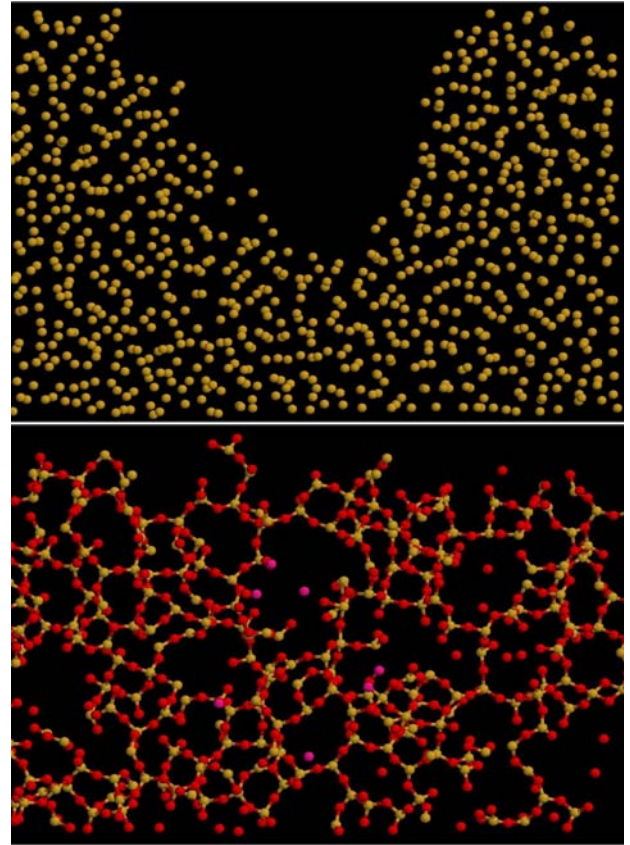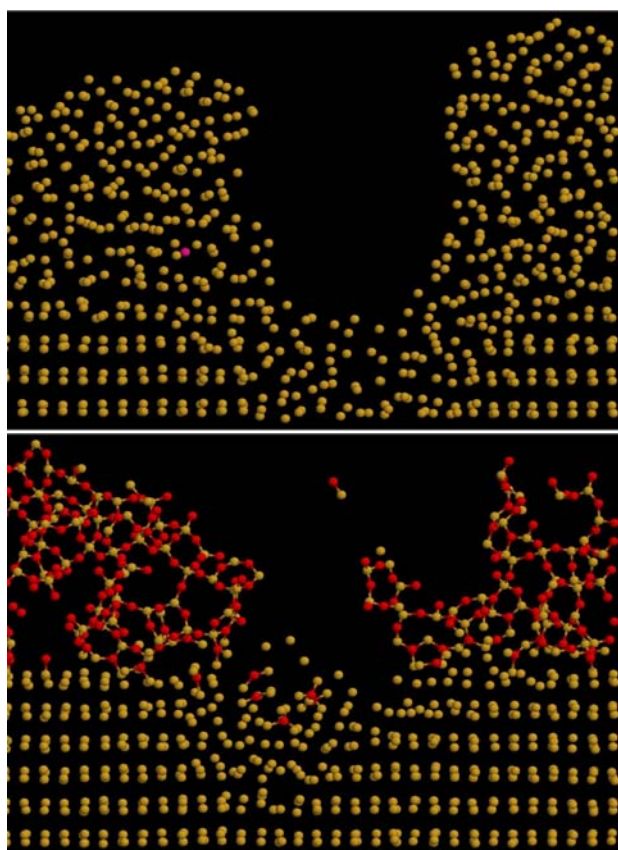

Fig. 1. (Color online) Examples of craters in a-Si and a-SiO$_2$. The vertical size of the slice in this and in the other visualizations is 4 nm, the horizontal size 6 nm and the thickness 1 nm.

Table 2. The average depth (range) of the argon atoms penetrating inside the target and number of displaced target atoms. Atoms that have moved more than 0.2 nm up or down from their original positions are included. The values are averages of five simulations.

Target	Ar range (nm)	Displaced atoms
c-Si	2.3 ± 1.5	830 ± 20
a-Si	2.4 ± 1.6	1490 ± 50
a-Si/c-Si	2.5 ± 0.6	5790 ± 140
c-SiO$_2$	8.0 ± 0.3	1730 ± 80
a-SiO$_2$	8.0 ± 0.3	2560 ± 40
a-SiO$_2$/c-Si	10.3 ± 0.4	1120 ± 20
Graphite	3.9 ± 0.1	n.a.

shown in Table 2. The corresponding depth profiles in Figure 2 show that atoms in a-SiO$_2$ are displaced both near the surface and deeper in the solid, whereas the displacement region in a-Si is more focused, which leads to a more localized damage. The network of tetrahedral SiO$_4$ modules mediates the impact energy to the environment more easily than the homogeneous a-Si structure. Comparison of c-Si and c-SiO$_2$ depth profiles in Figure 2 shows this even more clearly. In c-Si the cluster energy is released in a relatively small region around the impact point and a
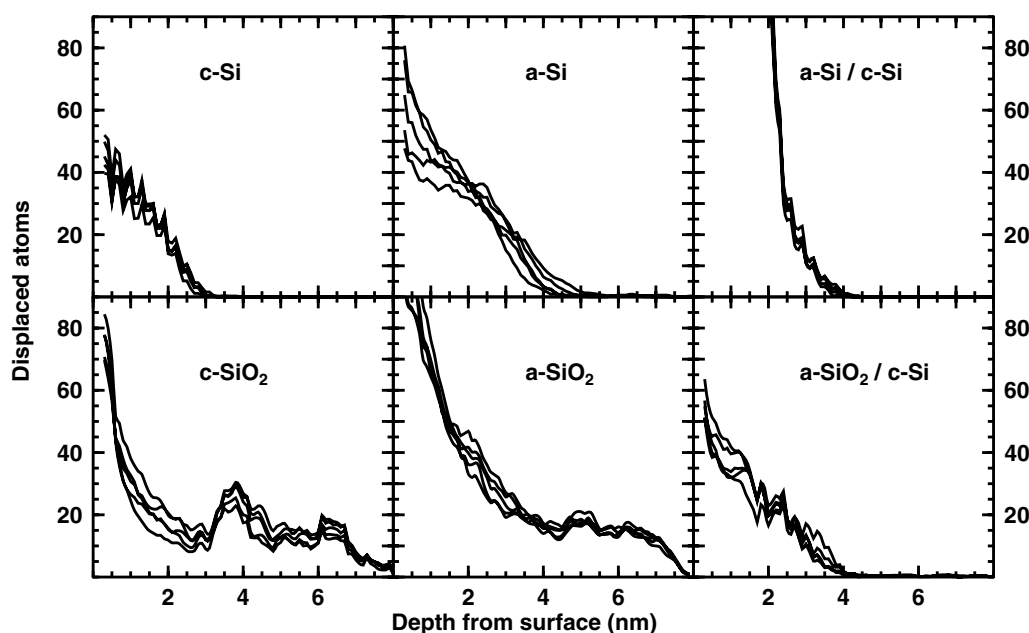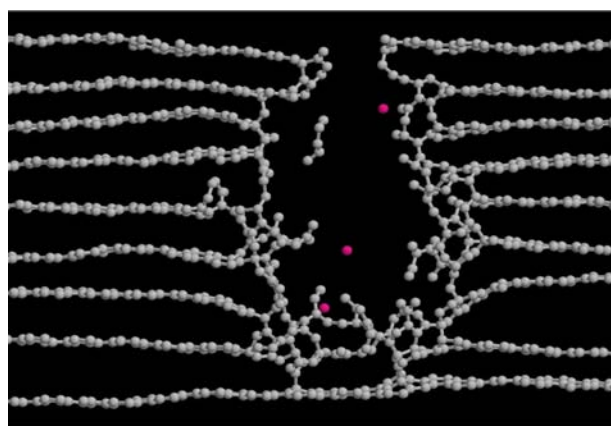
Fig. 2. Depth profiles of displaced atoms (number of atoms per Å). The corresponding profile of graphite is meaningless, because all atoms in the target are displaced due to the strong oscillations induced by the collision. Each curve shows the result of one simulation. The depth is calculated from the level of the original surface and atoms that have moved more than 0.2 nm up or down from their original positions are considered as displaced atoms.

Fig. 3. (Color online) Examples of craters in a-Si/c-Si and a-SiO$_2$/c-Si.

Fig. 4. (Color online) An example of a crater in graphite.

pure c-Si and a-SiO$_2$ targets. However, the comparison of depth profiles in Figure 2 and the comparison of numbers of displaced atoms in Table 2 shows that the a-SiO$_2$/c-Si layering decreases the number of displaced atoms, whereas in the a-Si/c-Si structure it increases the damage. Because the bottom crystalline layer is similar in both cases, this difference is a consequence of differences in collision dynamics between the 2 nm a-Si and a-SiO$_2$ layers.

The graphite structure responds very elastically to cluster impacts. Surface bump formation on ion implantation of graphite due to stresses developed in the near-surface layer was predicted earlier [17]. In contrast, the cratering on the graphite surface under Ar cluster impact was recently observed experimentally [18]. Figure 4 shows an example of a crater 40 ps after the collision in our simulations. The collisions induce oscillations of the lattice planes. The oscillations do not destroy the structure, although their amplitude could be as large as the distance between two graphite planes and they last at least 50 ps.

clear crater is created. In c-SiO$_2$ the crater is smaller but the cluster impact produces more defects.

The craters in a-Si/c-Si and a-SiO$_2$/c-Si structures (Fig. 3) are very much like combinations of the craters in

Only a small region of the graphite structure is destroyed by the 6 keV impact and a small crater is formed. In the early phases of the collision cascade the crater is larger, but the slightly damaged graphite layers in the bottom of the original crater can recover.

Also with the other structures, some recovering occurs. However, recovering effects, like smoothening of corners of surface structures, may take longer than it is in practice possible to simulate using molecular dynamics. Thus, it is possible that crater shapes observed with microscopy might be slightly different for that reason.

Table 2 shows that the range of Ar atoms is about three times longer in the silica structures than in the silicon structures. In addition, about half of the Ar atoms are sputtered from the silicon targets, whereas almost all Ar atoms are embedded in the silica structures. However, when c-Si is covered with a silica layer, the range of Ar is considerably longer and almost all Ar atoms are embedded into the c-Si layer. This occurs because the silica layer redirects the cluster atoms so that they are able to channel into Si lattice. In graphite, most of the Ar atoms are embedded and their average range is comparable to the ranges in the silicon structures. We can conclude, that the first graphite layers absorb the energy of the Ar atoms very effectively.

Although the short range electrostatic interactions are modelled in the silica potential used in this study [10,11], there are probably charge effects in the silica surface and the silica-silicon interface, which may affect the results of cluster impacts in reality. In the next phase the results of simulations will be compared with experimental data to verify whether or not this simple model of silica can be applied and what additional effects should be included in the simulation model.

4 Conclusions

Development of cluster radiation damage strongly depends on the material for the same cluster size and species, although the covalent bonding is the dominant bonding type in all the structures analyzed. In the case of c-Si or a-Si the damage is more localized and clear crater formation is observed compared to a-SiO_2. On the other hand, the projected ranges of cluster constituents are more than three times higher in SiO_2 compared to Si. The presence of a thin SiO_2 layer on the top of a Si target changes the projectile ranges and affects the crater shapes. The results demonstrate that MD simulations of multi-layer structures can give insights into mechanisms that might be important in understanding cluster impact and developing applications of cluster beams.

References

1. Y. Yamaguchi, J. Gspann, Eur. Phys. J. D **34**, 247 (2005)
2. P.W. Henkes, R. Klingelhöfer, Vacuum **39**, 541 (1989)
3. J. Gspann, Nucl. Instr. Meth. Phys. Res. B **80** (1993)
4. G. Brauchle, S. Richard-Schneider, D. Illig, J. Rockenberger, R.D. Beck, M.M. Kappes, Appl. Phys. Lett. **67**, 52 (1995)
5. L.P. Allen, Z. Insepov, D.B. Brenner, C. Santeufemio, W. Brooks, K.S. Jones, I. Yamada, J. Appl. Phys. **92**, 3671 (2002)
6. V. Popok, S. Prasalovich, E. Campbell, Surf. Sci. **556**, 1179 (2004)
7. J. Samela, K. Nordlund, J. Keinonen, V.N. Popok, Nucl. Instr. Meth. Phys. Res. B **255**, 253 (2007)
8. J. Samela, J. Kotakoski, K. Nordlund, J. Keinonen, Nucl. Instr. Meth. Phys. Res. B **239**, 331 (2005)
9. R. Vink, G. Barkemay, W. van der Wegz, N. Mousseaux, J. Non-Cryst. Solids **282**, 248 (2001)
10. H. Ohta, S. Hamaguchi, J. Chem. Phys. **115**, 6679 (2001)
11. T. Watanabe, H. Fujiwara, H. Noguchi, T. Hosino, I. Ohdomari, Jpn. J. Appl. Phys. Lett. **38**, 366 (1999)
12. T. Watanabea, D. Yamasakia, K. Tatsumuraa, I. Ohdomari, Appl. Surf. Sci. **234**, 207 (2004)
13. R.L.C. Vink, G.T. Barkema, Phys. Rev. B **67**, 245201 (2003)
14. D. Grimley, A. Wright, R. Sinclair, J. Non-Cryst. Solids **110**, 49 (1990)
15. K. Nordlund, J. Keinonen, T. Mattila, Phys. Rev. Lett. **77**, 699 (1996)
16. J.F. Ziegler, J.P. Biersack, U. Littmark, *The Stopping and Range of Ions in Matter* (Pergamon, New York, 1985)
17. A. Gras-Martí, R. Smith, K. Beardmore, V.K. José, J. Jiménez-Rodríguez, J. Ferrón, Comp. Mat. Sci. **3**, 413 (1995)
18. N. Toyoda, S. Houzumi, I. Yamada, Nucl. Instr. Meth. Phys. Res. B **241**, 609 (2005)